

Ionization potentials and dissociation energies of neutral, singly and doubly charged C_n fullerenes from $n = 20$ to 70

Sergio Díaz-Tendero, Goar Sánchez, Manuel Alcamí, Fernando Martín*

Departamento de Química, C-9, Universidad Autónoma de Madrid, 28049 Madrid, Spain

Received 21 October 2005; accepted 14 November 2005

Available online 23 March 2006

Abstract

Using B3LYP density functional theory, first and second ionization potentials as well as dissociation energies for neutral, singly and doubly charged fullerenes with sizes between 20 and 70 atoms have been evaluated. Comparison with available experimental data is good except for the doubly charged species. The results show that neutral fullerenes with a magic number of atoms, namely C_{32} , C_{50} , C_{60} and C_{70} , have the largest stability against ionization and C_2 evaporation. A similar large stability is observed for the corresponding singly and doubly charged magic fullerenes, except for C_{32}^+ and C_{32}^{2+} . Neutral and positively charged C_{62} is found to be rather unstable. Also, C_2^+ emission is shown to become competitive with C_2 emission for sufficiently small doubly charged fullerenes. The origin of these and other properties is discussed in detail. © 2006 Elsevier B.V. All rights reserved.

PACS: 36.40.Qv

Keywords: Fullerenes; Dissociation energy; Ionization potential; DFT calculations

1. Introduction

A large number of experimental and theoretical works have been devoted to understand the stability of the C_{60} fullerene in a variety of collision reactions (see Refs. [1,2] for recent reviews on the subject). Hot neutral C_{60} produced in these collisions can cool down by different competitive processes including emission of photons (radiative decay), electron emission (delayed ionization or *thermionic emission*) and evaporation of neutral fragments (dissociative decay) [3]:



The first process (1) consists in a cluster cooling through optical emission similar to the black-body radiation. The electron emission (2) can occur when the ionization potential is lower than the dissociation energy required to evaporate C_2 . In this

case, three different mechanisms have been observed: (i) direct ionization (without any relaxation time after the collision), (ii) statistical ionization resulting from a multiply excited electronic state and (iii) statistical ionization that is produced when the excess energy is relaxed into the vibrational modes [4]. The corresponding ionization timescales and the statistical electron emission problems have been recently reviewed [5,6].

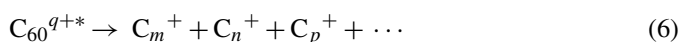
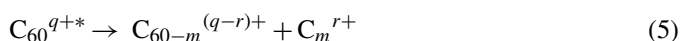
The third competitive process is the evaporation of neutral carbon dimers. In this context, it is commonly accepted that the dominant fragmentation channel of excited C_{60} (or C_{60}^+) involves sequential emission of C_2 units [7]. Experimentally, the dissociation energy of C_{60} into C_{58} and C_2 is determined from that of C_{60}^+ by using the difference in the ionization potentials of C_{60} and C_{58} (0.54 eV) [8,9]. The value of this dissociation energy has been the subject of intense controversy and debate for almost a decade (see Refs. [7,10] for reviews and a historical perspective on this subject). Until 1997 [11], most experimentalists believed that the dissociation energy of C_{60} was around 7–8 eV, while theoretical investigations predicted a value around 12 eV (see Ref. [12] and references therein). An explanation for this discrepancy has only been found in 2001 when researchers realized that the value of the Gspann parameter used in earlier experiments was too low [10]. The most recent experimental

* Corresponding author.

E-mail address: fernando.martin@uam.es (F. Martín).

determinations and the old ones corrected by using a more accurate value of the Gspann factor now agree with ab initio (MP2) and density functional theory (DFT) calculations in a value of the dissociation energy around 10–12 eV. Nevertheless, there are still some uncertainties associated with the value of the Gspann factor [13] and, in particular, whether or not the value of the factor deduced for C₆₀ is valid for smaller fullerenes.

For multiply charged C₆₀^{q+} fullerenes, the dominant decay channel is fragmentation. In this case, the fragmentation patterns extremely depend on the initial charge state *q*, and not only on their excitation energy *E*^{*} (see, e.g., [14–16]). Variations in these quantities (*q* and *E*^{*}) lead to very different decay channels: (i) successive emission of neutral C₂ molecules, (ii) fragmentation into one or more light charged clusters and (iii) fragmentation in several singly charged fragments with small masses:



These three processes are, respectively, known as sequential evaporation (4), asymmetric fission (5) and multifragmentation (6). In order to understand such decay processes, multiply charged fullerenes have been produced in collisions of C₆₀ and C₇₀ with fast highly charged ions [15–37], electrons [38–49] and intense laser pulses [50–55]. In these experiments, the knowledge of the dissociation energies and ionization potentials of all fragments is essential to analyze the observed fragmentation patterns. A fairly large number of theoretical works have been devoted to obtain such information for small carbon clusters (typically, with less than 10 atoms; see, e.g., [56] and references therein). However, only a few theoretical works have been reported for multiply charged fullerenes, and most of them have exclusively focused on C₆₀^{q+} [57–62]. In the latter case, an interesting theoretical conclusion is that *q* = 14 is the largest charge a C₆₀ fullerene can sustain against Coulomb explosion [61,62], which is consistent with the highest charge ever observed experimentally (*q* = 12, see Ref. [55]).

There have been some experimental attempts to determine dissociation energies and ionization potentials of fullerenes smaller or larger than C₆₀, either neutral or positively charged [39,40,63–66]. Very recently, the C₂ dissociation energy of C_{*n*}⁺ fullerenes (42 ≤ *n* ≤ 70) have been measured by Concina et al. using a three-sector-field mass spectrometer [67]. From the theoretical side, the most complete calculations of dissociation energies for fullerenes other than C₆₀ have been reported by Zhang et al. [68,69], Díaz-Tendero et al. [70] and Sánchez et al. [71]. In the early work of Refs. [68,69], only neutral species were considered. Dissociation energies for fullerenes as small as C₂₀ were determined by using a tight-binding model combined with a scheme to generate energetically favorable structures. In Ref. [70], the structure of neutral, singly and doubly charged C_{*n*} fullerenes with 50 < *n* < 60 was determined by performing geometry optimizations using B3LYP density functional theory. From the optimized geometries, dissociation energies and ionization potentials were obtained for the most stable fullerene isomers.

The work of Ref. [71] extended the above calculations to the size range 40 < *n* < 70, but only for neutral and singly charged species. Neutral fullerenes in the range 20 < *n* < 36 have been recently studied at different levels of theory [72]; however, no information is available for the corresponding singly and multiply charged species. The available structural properties and the reactivity of fullerenes with sizes between 20 and 60 have been recently reviewed in Ref. [73].

In this work, we have further extended the calculations reported in Refs. [70] and [71] to provide ionization potentials and dissociation energies for neutral, singly and doubly charged C_{*n*} fullerenes for sizes ranging from *n* = 20 to 70. This range covers all known fullerenes smaller than C₇₀. In addition to C₂ emission, we have also considered emission of C₂⁺, which may be a competitive process for the smaller fullerenes. As in Refs. [70] and [71], we have performed high level B3LYP density functional theory calculations to determine the geometry and the electronic energy of the most stable isomer for each size. The paper is organized as follows. In the next section, we briefly describe the theoretical methods used in this work. Our results on ionization potentials and dissociation energies are given and discussed in Section 3. Comparison with the available experimental measurements is also shown. We end with some conclusions in Section 4.

2. Computational details

We have employed in our calculations the density functional theory (DFT) with the B3LYP functional for exchange and correlation. This functional combines the Becke's three parameter non-local hybrid exchange potential [74] with the non-local correlation functional of Lee et al. [75]. The geometries of all the structures have been optimized by using the 6-31G(d) basis set. The B3LYP functional has been proved to be good a choice for the description of carbon clusters [70]. In the case of small carbon clusters, the calculated geometries and the vibrational frequencies are very close to those obtained at higher levels of theory [76,77,56]. The calculations have been carried out with the Gaussian 98 program [78]. The starting geometry of the classical structures investigated have been obtained with the help of the CaGe program [79].

3. Results and discussion

3.1. Isomer selection

The cage of a classical fullerene only contains pentagonal and hexagonal faces. According to Euler's theorem of polyhedra, each fullerene should have exactly 12 pentagons and an arbitrary number of hexagons. For a given size (i.e., for a given number of hexagons), there are many possible arrangements of pentagons and hexagons [80,81]. Therefore, the selection of the appropriate arrangement is actually the first difficulty one meets in the search for the most stable isomer. The relative position of the pentagonal faces determines the ring strain in the cage and, therefore, its stability. In general, the larger the number of adjacent pentagons (AP), the larger the strain. Thus, the most

stable fullerenes have all pentagons isolated, which is known as the isolated pentagon rule (IPR) [82]. Only C_{60} and fullerenes with a number of atoms equal or greater than 70 present isomers that follow the IPR. For other fullerenes, it is impossible to have all pentagons isolated. In this case, the most stable isomer is expected to have the lowest number of APs [83–85]. This second rule is known as the pentagon adjacency penalty rule (PAPR) or minimum pentagon-adjacency rule [82,85–88].

The fullerene C_{20} is the smallest classical structure one can construct, presenting 12 pentagons and no hexagons. Previous studies have evaluated the relative stability of this isomer with respect to other possible arrangements (e.g., ring and bowl) [89–93]. Here, we are interested in fullerenes and the other proposed structures for C_{20} are beyond the scope of the present work. It is not possible to construct a classical fullerene (with pentagons and hexagons) with 22 vertex (carbon atoms). Thus, the next fullerenes in the series are C_{24} and C_{26} (with only one classical isomer), C_{28} , C_{30} , etc.

In this work, we have followed a systematic procedure to find the most stable classical isomers for a given fullerene size. For sizes from $n=20$ to 34, we have considered all possible classical structures made of pentagons and hexagons (the only exceptions are C_{32}^+ and C_{32}^{2+} , for which only structures with the lowest number of APs have been considered). For larger sizes, we have considered all structures with the minimum number of APs but also some other classical structures with a larger number of APs and a few non-classical structures containing heptagons and/or squares that result from extraction or addition of C_2 units from the most stable isomers of neighboring size. Details of the criteria used to select the structures and specific examples in the range $n=52$ –60 can be found in Ref. [70].

Some exceptions to the PAPR have been found for both neutral and positively charged fullerenes [94–98]. In particular, Díaz-Tendero et al. [94] have shown using MP2 theory that C_{50} does not follow the PAPR (see also [95,96,98]): the isomer $C_{50}(D_3)$ containing 6 APs is 21.4 kcal/mol more stable than the isomer $C_{50}(D_{5h})$ containing 5 APs. At the B3LYP/6-31G(d) level of theory used in this work, $C_{50}(D_3)$ is only 2.3 kcal/mol more stable, in agreement with [94–96,98]. For positively charged species, the situation is the opposite. For instance, for the singly charged C_{50}^+ fullerene, the D_{5h} isomer is 9.5 kcal/mol more stable than the D_3 one and, therefore, the PAPR is fulfilled. A second example of fullerene that does not follow the PAPR is C_{52}^{2+} [97]. In this case, the calculations show again that, although there exists an isomer with 5 APs, the most stable structure present 6 APs [97]. In the neutral and singly charged C_{52} , the PAPR is fulfilled. These two exceptions have been explained in Refs. [97,94] as resulting from the larger sphericity of the isomer containing 6 APs. Indeed, both C_{50} and C_{52}^{2+} fullerenes have 50π electrons. In a spherical electronic model of fullerenes, C_{50} and C_{52}^{2+} have a closed electronic shell with $2(l+1)^2 \pi$ electrons ($l=4$), which results in spherical aromaticity and, therefore, in additional stability [99,94]. This surplus of stability can compensate the additional strain due to a larger number of adjacent pentagons. In summary, for fullerenes satisfying the $2(l+1)^2$ rule, the larger the sphericity, the more stable the corresponding isomer. Other fullerenes that follow the

$2(l+1)^2$ rule in the size range investigated in this work are C_{32} and C_{34}^{2+} ($l=3$). However, no exception to the PAPR has been found in these cases because the most spherical shapes always correspond to the isomers with the minimum number of APs.

For C_{62} , Sánchez et al. have shown that two non-classical structures are more stable than the classical ones [71]. In particular, an isomer of C_{2v} symmetry containing a square ring is ~ 10.4 kcal/mol more stable than the most stable classical isomer. The structure containing the square ring has been proposed in Ref. [100] and it has been recently synthesized [101]. We have also found that a second non-classical isomer proposed by Ayuela et al. [87] containing a heptagon is even more stable: it has C_s symmetry and its energy is ~ 13.5 kcal/mol lower than that of the most stable classical fullerene. In the case of the positively charged species, the latter isomer is even more stable: 10.2 and 17.7 kcal/mol, respectively. It is worth mentioning, that only extraction of C_2 dimers from the non-classical structures containing either the square or the heptagon leads to the well known icosahedral isomer of C_{60} ; extraction of C_2 from classical C_{62} isomers lead to C_{60} isomers containing either adjacent pentagons or non-classical rings.

We present in Fig. 1 the two-dimensional projections of the most stable isomers found at the B3LYP/6-31G(d) level of theory for each fullerene size. For the sake of clarity we have filled with different patterns the adjacent and the isolated pentagons, as well as the non-classical rings. In the same figure, we have included the symmetry as provided by the CaGe program. This is the fullerene symmetry before geometry optimization is performed. For a few positively charged fullerenes, the most stable isomer is not the same as for neutrals ($n=48, 50, 52, 66$ and 68). For these exceptions, we have also included in the bottom of the figure the projections of the corresponding C_n^+ and/or C_n^{2+} isomers. Isomers with the same number of APs can be nearly degenerate. In this case, one can expect inversions in energy when different theoretical methods are used. These special cases have been recently reviewed by Lu and Chen [73]. A summary of the structure information of all fullerenes is given in the first four columns of Table 1.

A visual inspection of Fig. 1 and Table 1 shows that the number of adjacent pentagons decreases with fullerene size. We can also see that, when possible, the adjacent pentagons are preferentially arranged in chains. In order to minimize the ring strain these chains are as small as possible. A more detailed analysis of the structure of the different isomers studied in this work will be presented elsewhere [102].

3.2. Ionization potentials

We have used the absolute electronic energies of the most stable isomers to evaluate the first and second adiabatic ionization potentials (IP) of C_n fullerenes. The ionization potentials have been obtained by subtracting the absolute energies of C_n^+ and C_n^{2+} (for the first IP) and those of C_n^+ and C_n^{2+} (for the second IP) in their optimum geometries. In all cases but five, C_n, C_n^+ and C_n^{2+} have the same isomeric form (see Fig. 1 and Table 1) and, therefore, there is no ambiguity. For $C_{48}, C_{50}, C_{52}, C_{66}$ and C_{68} the isomeric form of the neutral species differs from that of the

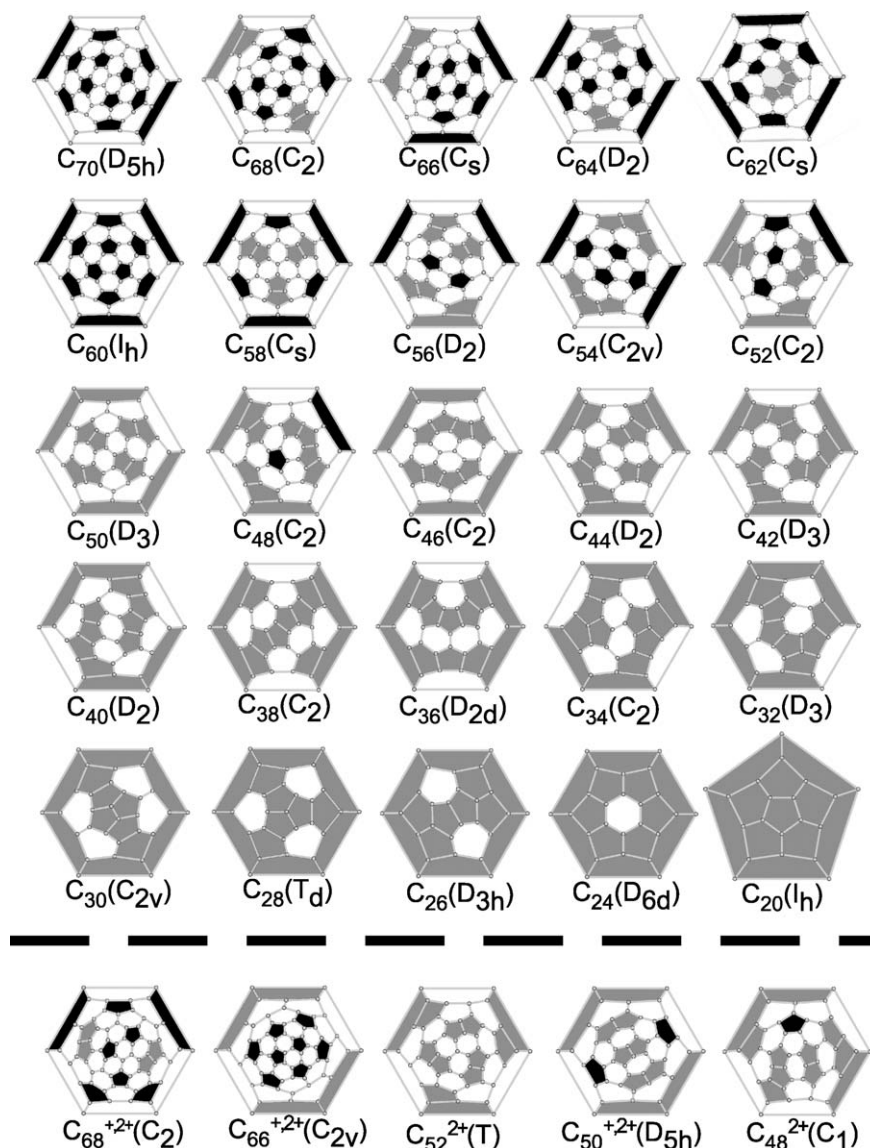


Fig. 1. Two-dimensional projections of the most stable isomers of C_n^{q+} fullerenes. Isolated and adjacent pentagons have been filled using different patterns. An heptagonal ring in C_{62} has been also filled. The symmetry as given by the CaGe program [79] is also shown (i.e., before geometry optimization). As a general trend, the most stable isomer of the charged species is same as for neutrals. Exceptions are shown in the last row.

charged one. In these five cases, we have used, for the positively charged species, the energies of the isomeric forms that have the same atomic arrangement as the neutral species. This implies that no bond breaking is allowed during the ionization process, but bond relaxation is always included. Therefore, the calculated ionization potentials should be considered as adiabatic.

Table 1 and Fig. 2 show our results for the first and second ionization potentials of C_n fullerenes as functions of cluster size. Fig. 2 also includes the experimental data of Refs. [103,107] for the first and second IPs. Our results are in good agreement with the experimental data, except for a constant downward shift of ~ 0.5 eV in the case of the first IP. The first IP exhibits maxima for the magic number fullerenes C_{32} , C_{50} , C_{60} and C_{70} . These fullerenes are significantly more stable than their neighbors. The large stability of C_{60} and C_{70} is due to the absence of adjacent pentagons in the cage, which implies low ring strain (fullerenes

between C_{60} and C_{70} always have APs). In addition, C_{60} is nearly spherical (I_h symmetry), which provides a surplus of stability. C_{50} is the smallest fullerene in which pentagons can be arranged in pairs of APs (smaller fullerenes always have chains of three or more adjacent pentagons). In addition, as explained above, it follows the $2(l+1)^2$ rule and, therefore, has spherical aromaticity. The latter effect also explains the large stability of C_{32} . The larger stability of C_{32} with respect to other sizes has been also predicted by Kietzmann et al. [108].

The case of C_{50} deserves a more extended analysis. As mentioned above and discussed in [94], the most stable C_{50} isomer has D_3 symmetry and does not follow the PAPR. Therefore, the theoretical value given in Fig. 2 (and Table 1) corresponds to the $C_{50}(D_3) \rightarrow C_{50}^+(D_3) + e^-$ ionization process. However, if we consider the ionization energy of the other isomer, i.e., $C_{50}(D_{5h}) \rightarrow C_{50}^+(D_{5h}) + e^-$, one obtains a value of 6.75 eV

Table 1

Symmetry (before geometry optimization), structure (namely ring structures different from hexagons and isolated pentagons), number of adjacent pentagons (NAP), first and second adiabatic ionization potentials (IP) in eV for the most stable fullerenes at the B3LYP/6-31G(d) level of theory

C_n	Symmetry	Structure	NAP	First IP (eV)	Second IP (eV)
C_{70}	D_{5h}	–	0	7.02	10.00
C_{68}	$C_2 (C_2)^{+,2+}$	2-2AP (2-2AP) ^{+,2+}	2* (2) ^{+,2+,*}	6.87	10.04
C_{66}	$C_s (C_{2v})^{+,2+}$	1-C3AP (2-2AP) ^{+,2+}	2* (2) ^{+,2+,*}	6.86	9.98
C_{64}	D_2	2-2AP	2*	6.78	9.94
C_{62}	C_s	1Hp + 1-C4AP	3 + Hp*	6.36	9.90
C_{60}	I_h	–	0	7.14	10.37
C_{58}	C_s	3-2AP	3	6.41	9.91
C_{56}	D_2	4-2AP	4*	6.65	10.01
C_{54}	C_{2v}	2-C3AP	4	6.61	10.13
C_{52}	$C_2 (T)^{2+}$	2-C3AP + 1-2AP (6-2AP) ²⁺	5 (6) ^{2+,*}	6.54	10.10
C_{50}	$D_3 (D_{5h})^{+,2+}$	6-2AP (5-2AP) ^{+,2+}	6* (5) ^{+,2+}	7.26	10.86
C_{48}	$C_2 (C_1)^{2+}$	1-C4AP + 2-C3AP (1-AP + 3-C3AP) ²⁺	7* (7) ^{2+,*}	6.85	10.49
C_{46}	C_2	2-C4AP + 2-2AP	8*	7.04	10.74
C_{44}	D_2	2-C4AP + 2-2AP	8*	7.15	10.90
C_{42}	D_3	3-C4AP	9	7.13	10.88
C_{40}	D_2	2-C6AP	10*	7.01	10.82
C_{38}	C_2	1-C11AP	11	6.79	10.78
C_{36}	D_{2d}	2-C4AH	12*	6.40	10.47
C_{34}	C_2	1-C3AH + 1-C4AH	14	6.70	10.80
C_{32}	D_3	3-2AH	15	7.62	10.70
C_{30}	C_{2v}	2-2AH	17	7.16	11.59
C_{28}	T_d	3-IH	18	6.57	11.73
C_{26}	D_{3h}	2-IH	21	6.80	12.08
C_{24}	D_{6d}	1-IH	24	7.15	11.53
C_{20}	I_h	0-IH	30	6.59	11.46

Structures of neutral and singly charged species are generally the same; when they differ, those of the singly or doubly charged species are given within parenthesis with a superscript indicating the charge. *Notations*: 2AP, two adjacent pentagons; C3AP, a chain of three adjacent pentagons; 1Hp, a heptagon; C4AP, a chain of four adjacent pentagons; C6AP, a chain of six adjacent pentagons; C11AP, a chain of eleven adjacent pentagons. For fullerenes smaller than C_{38} , the notation refers to the number of hexagons (because they are fewer and most pentagons touch through multiple connections): AH, adjacent hexagon; IH, isolated hexagon. The asterisks (*) indicate that there are more isomers with the same number of adjacent pentagons (although their energy is higher).

(empty circle in Fig. 2), which is far away from the experimental value of Zimmerman et al. [103] and would not lead to a maximum in the IP curve. This comparison with experiment indicates that the D_3 isomer is indeed the one observed experimentally.

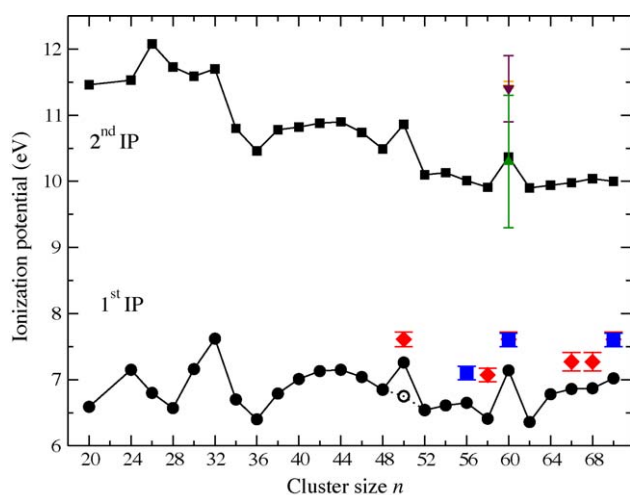


Fig. 2. Comparison between calculated and experimental first and second ionization potentials as functions of cluster size. Full circles, this work. Experimental values: diamonds, Zimmerman et al. [103]; squares, McElvany et al. [104], triangle up, Baba et al. [105]; triangle down, Muig et al. [106]; cross, Steger et al. [107]. Empty circle: result obtained for a C_{50} fullerene of D_{5h} symmetry (see text).

The second ionization potential roughly decreases with fullerene size. This is similar to what has been observed for small carbon clusters [56]. As expected, the corresponding curve presents maxima at $n = 60, 50$ and 32 . However, an additional peak appears at $n = 26$. This peak can also be understood in terms of electronic structure. Indeed, C_{26}^+ has 25π electrons. Using again the spherical electron gas model, the fourth shell ($l = 4$) is half filled, which, according to Hund's rule, provides an extra stability.

3.3. Dissociation energies

C_2 and C_2^+ dissociation energies of neutral, singly and doubly charged fullerenes have been evaluated using the electronic energies of the most stable isomers. The results are given in Table 2. For the calculation of C_2 dissociation energies, we have used the absolute energy of C_2 obtained at the same level of theory and corrected as explained in [70].

C_2 dissociation energies are very similar for neutral and positively charged species except in the size intervals $n = 58-64$ and $30-38$. Thus, similar qualitative trends are observed concerning their variation with cluster size.

Fig. 3 shows the C_2 dissociation energy of neutral fullerenes as a function of cluster size. Our results agree reasonably well with those of Zhang et al. [109,69]. The maximum dissociation energies correspond again to magic number fullerenes: C_{32}, C_{50} ,

Table 2
Dissociation energies (in eV) at the B3LYP/6-31G(d) level of theory

n	$C_n/(C_{n-2} + C_2)$	$C_n^+/(C_{n-2}^+ + C_2)$	$C_n^{2+}/(C_{n-2}^{2+} + C_2)(C_{n-2}^+ + C_2^+)$	
C ₇₀	10.36	10.1	9.44	11.96
C ₆₈	8.36	8.29	8.60	10.82
C ₆₆	7.88	7.97	8.26	10.18
C ₆₄	8.99	8.57	8.53	10.49
C ₆₂	5.53	6.31	6.77	8.27
C ₆₀	11.37	10.64	10.18	12.13
C ₅₈	8.11	8.35	8.45	10.30
C ₅₆	8.47	8.43	8.54	10.27
C ₅₄	8.44	8.37	7.96	10.10
C ₅₂	7.79	8.10	8.56	10.24
C ₅₀	9.63	9.63	9.92	11.31
C ₄₈	8.60	8.79	8.84	10.18
C ₄₆	7.79	7.90	8.11	9.24
C ₄₄	8.61	8.59	8.64	9.72
C ₄₂	8.50	8.38	8.42	9.46
C ₄₀	8.41	8.19	8.15	9.23
C ₃₈	8.41	8.02	7.71	9.10
C ₃₆	8.44	8.73	9.07	10.12
C ₃₄	7.41	8.33	9.23	9.38
C ₃₂	9.60	9.14	9.02	9.29
C ₃₀	8.94	8.36	8.50	8.62
C ₂₈	8.78	9.02	9.36	9.14
C ₂₆	8.01	8.35	7.81	8.13

C₆₀ and C₇₀. The lowest dissociation energy corresponds to C₆₂. In this case, the product of dissociation is the icosahedral C₆₀ fullerene. Therefore, it is not surprising that the energy required is smaller than for the other fullerenes.

Fig. 4 shows the dissociation energy for C₂ and C₂⁺ emission from singly charged C_n⁺ as a function of fullerene size. Absolute experimental values for C₂ emission [66,67,65] are also shown for comparison. Since the data of Barran et al. [63] were obtained in arbitrary units, they have been represented after renormalization to the value calculated for C₅₄⁺. Our results show the same trends as the experimental values, in particular the pronounced peaks observed in the vicinity of C₅₀⁺, C₆₀⁺ and C₇₀⁺, and the pronounced minimum for C₆₂⁺. For fullerenes with sizes $n \leq 38$, the C₂ dissociation energies oscillate with size. Also the maximum for C₃₂⁺ is not as pronounced as for the other magic sizes, which must be the consequence of the lack of spherical aromaticity since C₃₂⁺ has only 31 electrons instead of 32. The oscillations for $n \leq 38$ are less pronounced in the C₂⁺ dissociation energy, except for the deep minimum observed for C₃₄⁺. The origin of this minimum is the high stability of the resulting product C₃₂ (after emission of C₂⁺) compared to the less stable dissociation products of the neighbors. A similar effect, although much less pronounced, is observed for C₅₂⁺. As in the neutral case, the lowest dissociation energies correspond again to C₆₂⁺. If one takes the most stable classical isomer of C₆₂⁺ instead of that containing the heptagonal ring, one obtains dissociation energies for C₆₄⁺ and C₆₂⁺ that are, respectively, ~ 1 eV larger and smaller than those shown in Fig. 4. This would deteriorate the

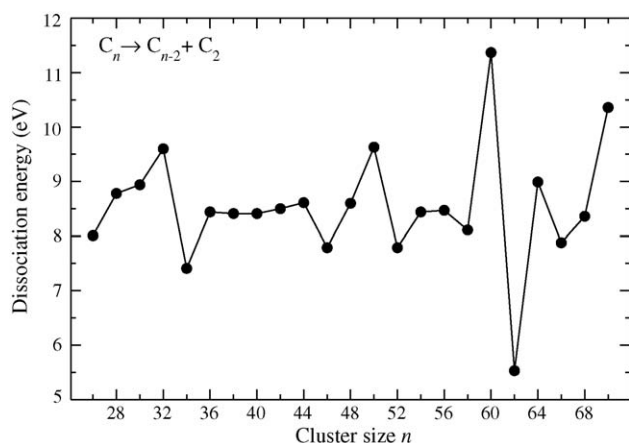


Fig. 3. C₂ dissociation energy as a function of cluster size for neutral fullerenes.

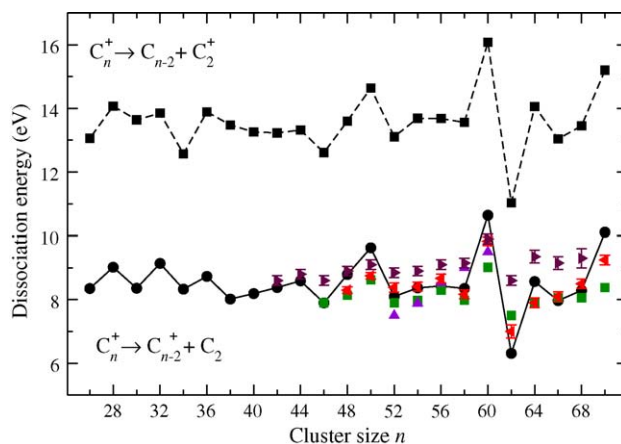


Fig. 4. C₂ (circles, full line) and C₂⁺ (squares, dashed line) dissociation energies as functions of fullerene size. Circles: this work. Experimental values for C₂ dissociation energies: squares, Barran et al. (Ref. [63]) scaled to C₅₄⁺; triangles up, Laskin et al. (Ref. [65]); triangles left, Tomita et al. (Ref. [66]); triangles right, Concina et al. (Ref. [67]).

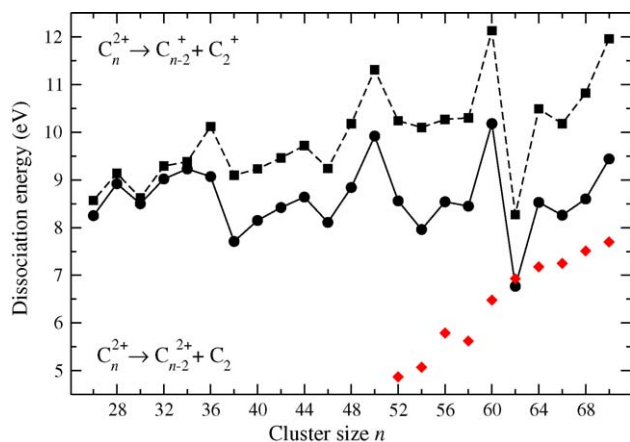


Fig. 5. C_2 (circles, full line) and C_2^+ (squares, dashed line) dissociation energies as functions of cluster size for doubly charged fullerenes. The experimental results for C_2 dissociation energies (diamonds) have been taken from Ref. [38].

agreement with experiment, which proves that the C_{62}^+ fullerene obtained in the experiments is indeed a non-classical structure as that considered in the present work.

Fig. 5 shows C_2 and C_2^+ dissociation energies for the doubly charged fullerenes. The C_2^{2+} dissociation energy is always much larger than the C_2 or C_2^+ ones (~ 25 – 30 eV) and, for this reason, they are not shown in the figure. The comparison with the only available experimental data [38] is not good for $n \leq 60$. Again maxima are observed for $n = 50, 60$ and 70 . However, in this case, the fluctuations with size are less pronounced than in singly charged and neutral fullerenes. We can also see that the C_2^+ dissociation energy is close to the C_2 one for the smaller fullerenes ($n \leq 34$). The sudden decrease of the C_2^+ dissociation energy for $n \leq 34$ can be explained by the fact that it is more convenient to split the charge between two small fragments than locating it in a single small fragment. This implies that, for small fullerenes, one can expect asymmetric fission ($C_n^{2+} \rightarrow C_{n-2}^+ + C_2^+$) to compete with C_2 evaporation ($C_n^{2+} \rightarrow C_{n-2}^{2+} + C_2$) even for relatively cold C_n^{2+} ions. It is worth noticing the presence of a small maximum in the C_2 dissociation energy at $n = 34$ and not at $n = 32$ as for the neutral and singly charged fullerenes. This is because C_{34}^{2+} has the right number of electrons (namely, 32) to exhibit spherical aromaticity.

Such an effect is not observed in the case of C_2^+ emission because it is hidden by the sudden decrease in the corresponding dissociation energy. In the case of C_{52}^{2+} , which also exhibits spherical aromaticity, no singular behavior is observed either.

4. Conclusions

We have evaluated the electronic energies of neutral, singly and doubly charged fullerenes from C_{20} to C_{70} using B3LYP density functional theory at the 6-31G(d) level. The geometries of the most stable species have been fully optimized at the same level of theory. From these results, we have evaluated first and second ionization potentials of neutral fullerenes as well as dissociation energies of neutral, singly and doubly charged fullerenes. Comparison with the available experimental data is fairly good except for doubly charged species. We have found

that neutral fullerenes with a magic number of atoms, namely C_{32}, C_{50}, C_{60} and C_{70} , have the largest stability against ionization and C_2 evaporation. For the former two, the stability is partly due to spherical aromaticity, while, for the other two, it is mainly due to the absence of adjacent pentagons in the fullerene cage. We have found a similar large stability for the corresponding singly and doubly charged magic fullerenes, except for C_{32}^+ and C_{32}^{2+} due to the loss of spherical aromaticity. Although spherical aromaticity is also lost in C_{50}^+ and C_{50}^{2+} , these ionic species are still very stable because all pentagons in the fullerene cages are distributed in pairs of adjacent pentagons isolated from each other. We have also found that C_{32}^{2+} is rather stable because it presents spherical aromaticity. The results show that neutral and positively charged C_{62} is significantly more unstable than its neighbors. This is because emission of a carbon dimer leads to the very stable C_{60} fullerene in its almost perfect spherical shape. Similarly, C_{34}^+ is rather unstable against C_2^+ emission because the latter process leads to a very stable C_{32} fragment with spherical aromaticity. Finally, we have found that asymmetric fission of small doubly charged fullerenes (i.e., C_2^+ emission) efficiently competes with C_2 evaporation.

The optimized geometries and electronic energies of all the fullerenes considered in this work are available through the web at <http://www.uam.es/departamentos/ciencias/quimica/spline/fullerenes/>.

Acknowledgments

We thank the CCC-UAM and CIEMAT for allocation of computer time. Work partially supported by the DGI project Nos. BFM2003-00194, BQU2003-00894 and CTQ2004-00039/BQU, and the CAM project No. GR/MAT/0083/2004.

References

- [1] E.E.B. Campbell, F. Rohmund, Rep. Prog. Phys. 63 (2000) 1061.
- [2] E.E. Campbell, Fullerene Collision Reactions, first ed., Kluwer Academic Publishers, Dordrecht, 2003.
- [3] C. Lifshitz, Int. J. Mass Spectrom. 200 (2000) 423.
- [4] K. Hansen, K. Hoffmann, E.E.B. Campbell, J. Chem. Phys. 119 (2003) 2513.
- [5] E.E.B. Campbell, R.D. Levine, Annu. Rev. Phys. Chem. 51 (2000) 65.
- [6] J.U. Andersen, E. Bonderup, K. Hansen, J. Phys. B 35 (2002) R1.
- [7] C. Lifshitz, Int. J. Mass Spectrom. 198 (2000) 1.
- [8] P. Sandler, C. Lifshitz, C.E. Klots, Chem. Phys. Lett. 200 (1992) 445.
- [9] C. Lifshitz, Mass Spectrom. Rev. 12 (1993) 261.
- [10] S. Matt, O. Echt, P. Scheier, T.D. Märk, Chem. Phys. Lett. 348 (2001) 194.
- [11] K. Hansen, O. Echt, Phys. Rev. Lett. 78 (1997) 2337.
- [12] A.D. Boese, G.E. Scuseria, Chem. Phys. Lett. 294 (1998) 233.
- [13] K. Hansen, E.E.B. Campbell, Int. J. Mass Spectrom. 233 (2004) 215.
- [14] A. Rentenier, D. Bordenave-Montesquieu, P. Moretto-Capelle, A. Bordenave-Montesquieu, J. Phys. B 36 (2003) 1585.
- [15] A. Reinkoster, U. Werner, N.M. Kabachnik, H.O. Lutz, Phys. Rev. A 64 (2001) 032703.
- [16] S. Martín, L. Chen, A. Denis, R. Bredy, J. Bernard, J. Desesquelles, Phys. Rev. A 62 (2000) 022707.
- [17] S.H. Schwartz, A. Fardi, K. Haghigat, A. Langereis, H.T. Schmidt, H. Cederquist, Phys. Rev. A 63 (2000) 013201.
- [18] L. Chen, S. Martín, R. Bredy, J. Bernard, J. Desesquelles, Phys. Rev. A 64 (2001) 031201(R).

- [19] L. Chen, J. Bernard, G. Berry, R. Bredy, J. Desesquelles, S. Martín, *Phys. Scr.* T92 (2001) 138.
- [20] S. Tomita, H. Lebius, A. Brenac, F. Chandezon, B.A. Huber, *Phys. Rev. A* 65 (2002) 053201.
- [21] S. Matt, B. Dünser, M. Lezius, H. Deutsch, K. Becker, A. Stamatovic, P. Scheier, T.D. Märk, *J. Chem. Phys.* 105 (1996) 1880.
- [22] T. Lebrun, H.G. Berry, S. Cheng, R.W. Dunford, H. Esbensen, D.S. Gemmell, E.P. Kanter, W. Bauer, *Phys. Rev. Lett.* 72 (1994) 3965.
- [23] S. Cheng, H.G. Berry, R.W. Dunford, H. Esbensen, D.S. Gemmell, E.P. Kanter, T. LeBrun, W. Bauer, *Phys. Rev. A* 54 (1996) 3182.
- [24] Y. Nakai, T. Kambara, A. Itoh, H. Tsuchida, Y. Yamazaki, *Phys. Rev. A* 64 (2001) 043205.
- [25] P. Moretto-Capelle, D. Bordenave-Montesquieu, A. Rentenier, A. Bordenave-Montesquieu, *J. Phys. B* 34 (2001) L611.
- [26] T. Schlatholter, R. Hoekstra, R. Morgenstern, *J. Phys. B* 31 (1998) 1321.
- [27] A. Itoh, H. Tsuchida, T. Majima, S. Anada, A. Yogo, N. Imanishi, *Phys. Rev. A* 6001 (2000) 2702.
- [28] A. Itoh, H. Tsuchida, T. Majima, N. Imanishi, *Phys. Rev. A* 59 (1999) 4428.
- [29] A. Itoh, H. Tsuchida, K. Miyabe, T. Majima, Y. Nakai, *Phys. Rev. A* 64 (2001) 032703.
- [30] H. Tsuchida, A. Itoh, Y. Nakai, K. Miyabe, N. Imanishi, *J. Phys. B* 31 (1998) 5383.
- [31] A. Reinkoster, U. Werner, H.O. Lutz, *Eur. Phys. Lett.* 43 (1998) 653.
- [32] A. Langereis, J. Jensen, A. Fardi, K. Haghghat, H.T. Schmidt, S.H. Schwartz, H. Zettergren, H. Cederquist, *Phys. Rev. A* 63 (2001) 062725.
- [33] O. Hadjar, R. Hoekstra, R. Morgenstern, T. Schlatholter, *Phys. Rev. A* 63 (2001) 033201.
- [34] O. Hadjar, P. Foldi, R. Hoekstra, R. Morgenstern, T. Schlatholter, *Phys. Rev. Lett.* 84 (2000) 4076.
- [35] T. Schlatholter, O. Hadjar, R. Hoekstra, R. Morgenstern, *Phys. Rev. Lett.* 82 (1999) 73.
- [36] H. Cederquist, A. Fardi, K. Haghghat, A. Langereis, H.T. Schmidt, H. Schwartz, J.C. Levin, I.A. Sellin, H. Lebius, B. Huber, M.O. Larsson, P. Hvelplund, *Phys. Rev. A* 61 (2000) 022712.
- [37] T. Schlatholter, O. Hadjar, J. Manske, R. Hoekstra, R. Morgenstern, *Int. J. Mass Spectrom.* 192 (1999) 245.
- [38] S. Matt, O. Echt, T. Rauth, B. Dünser, M. Lezius, A. Stamatovic, P. Scheier, T.D. Märk, *Z. Phys. D* 40 (1997) 389.
- [39] S. Matt, O. Echt, R. Wörgötter, P. Scheier, C.E. Klots, T.D. Märk, *Int. J. Mass Spectrom.* 167 (1997) 753.
- [40] S. Matt, R. Parajuli, A. Stamatovic, P. Scheier, T.D. Märk, J. Laskin, C. Lifshitz, *Eur. Mass Spectrom.* 5 (1999) 477.
- [41] A. Itoh, H. Tsuchida, K. Miyabe, T. Majima, N. Imanishi, *J. Phys. B* 32 (1999) 277.
- [42] P. Scheier, B. Dünser, R. Wörgötter, M. Lezius, R. Robl, T.D. Märk, *Int. J. Mass Spectrom. Ion Process.* 138 (1994) 77.
- [43] P. Scheier, R. Robl, B. Schiestl, T.D. Märk, *Chem. Phys. Lett.* 220 (1994) 141.
- [44] P. Scheier, B. Dünser, R. Wörgötter, D. Muigg, S. Matt, O. Echt, M. Foltin, T.D. Märk, *Phys. Rev. Lett.* 77 (1996) 2654.
- [45] P. Scheier, T.D. Märk, *Int. J. Mass Spectrom. Ion Process.* 133 (1994) L5.
- [46] S. Matt, M. Sonderegger, R. David, O. Echt, P. Scheier, J. Laskin, C. Lifshitz, T.D. Märk, *Int. J. Mass Spectrom.* 187 (1999) 813.
- [47] M.O. Larsson, P. Hvelplund, M.C. Larsen, H. Shen, H. Cederquist, H.T. Schmidt, *Int. J. Mass Spectrom.* 177 (1998) 51.
- [48] D. Hathiramani, K. Aichele, W. Arnold, K. Huber, E. Salzborn, P. Scheier, *Phys. Rev. Lett.* 85 (2000) 3604.
- [49] P. Scheier, D. Hathiramani, W. Arnold, K. Huber, E. Salzborn, *Phys. Rev. Lett.* 84 (2000) 55.
- [50] E.E.B. Campbell, K. Hoffmann, H. Rottke, I.V. Hertel, *J. Chem. Phys.* 114 (2001) 1716.
- [51] E.E.B. Campbell, K. Hoffmann, I.V. Hertel, *Eur. Phys. J. D* 16 (2001) 345.
- [52] F. Rohmund, M. Heden, A.V. Bulgakov, E.E.B. Campbell, *J. Chem. Phys.* 115 (2001) 3068.
- [53] E.E.B. Campbell, K. Hansen, K. Hoffmann, G. Korn, M. Tchapyguine, M. Wittmann, I.V. Hertel, *Phys. Rev. Lett.* 84 (2000) 2128.
- [54] M. Tchapyguine, K. Hoffmann, O. Duhr, H. Hohmann, G. Korn, H. Rottke, M. Wittmann, I.V. Hertel, E.E.B. Campbell, *J. Chem. Phys.* 112 (2000) 2781.
- [55] V.R. Bhardwaj, P.B. Corkum, D.M. Rayner, *Phys. Rev. Lett.* 91 (2003) 203004.
- [56] S. Díaz-Tendero, F. Martín, M. Alcamí, *J. Phys. Chem. A* 106 (2002) 10782.
- [57] J. Cioslowski, S. Patchkovskii, W. Thiel, *Chem. Phys. Lett.* 248 (1996) 116.
- [58] T. Baştuğ, P. Kürpick, J. Meyer, W.-D. Sepp, B. Fricke, A. Rosén, *Phys. Rev. B* 55 (1997) 5015.
- [59] C. Yannouleas, U. Landman, *Chem. Phys. Lett.* 217 (1994) 175.
- [60] G. Seifert, R. Gutierrez, R. Schmidt, *Phys. Lett. A* 211 (1996) 357.
- [61] S. Díaz-Tendero, M. Alcamí, F. Martín, *Phys. Rev. Lett.* 95 (2005) 013401.
- [62] S. Díaz-Tendero, M. Alcamí, F. Martín, *J. Chem. Phys.* 123 (2005) 184306.
- [63] P.E. Barran, S. Firth, A.J. Stace, H.W. Kroto, K. Hansen, E.E.B. Campbell, *Int. J. Mass Spectrom.* 167 (1997) 127.
- [64] R. Wörgötter, B. Dünser, P. Scheier, T.D. Märk, M. Foltin, C.E. Klots, J. Laskin, C. Lifshitz, *J. Chem. Phys.* 104 (1996) 1225.
- [65] J. Laskin, B. Hadas, T.D. Märk, C. Lifshitz, *Int. J. Mass Spectrom.* 177 (1998) L9.
- [66] S. Tomita, J.U. Andersen, C. Gottrup, P. Hvelplund, U.V. Pedersen, *Phys. Rev. Lett.* 87 (2001) 073401.
- [67] B. Concina, K. Gluch, S. Matt-Leubner, O. Echt, P. Scheier, T.D. Märk, *Chem. Phys. Lett.* 407 (2005) 464.
- [68] B.L. Zhang, C.Z. Wang, C.T. Chan, K.M. Ho, *J. Phys. Chem.* 97 (1993) 3134.
- [69] B.L. Zhang, C.H. Xu, C.Z. Wang, C.T. Chan, K.M. Ho, *Phys. Rev. B* 46 (1992) 7333.
- [70] S. Díaz-Tendero, M. Alcamí, F. Martín, *J. Chem. Phys.* 119 (2003) 5545.
- [71] G. Sánchez, S. Díaz-Tendero, M. Alcamí, F. Martín, *Chem. Phys. Lett.* 416 (2005) 14.
- [72] G. Zheng, S. Irle, K. Morokuma, *Chem. Phys. Lett.* 412 (2005) 210.
- [73] X. Lu, Z. Chen, *Chem. Rev.* 105 (2005) 3643.
- [74] A.D. Becke, *J. Chem. Phys.* 98 (1993) 5648.
- [75] C. Lee, W. Yang, R.G. Parr, *Phys. Rev. B* 37 (1988) 785.
- [76] J.M.L. Martín, J. El-Yazal, J.P. Frangois, *Chem. Phys. Lett.* 242 (1995) 570.
- [77] J.M.L. Martín, J. El-Yazal, J.P. Frangois, *Chem. Phys. Lett.* 252 (1996) 9.
- [78] M.J. Frisch, G.W. Trucks, H.B. Schlegel, G.E. Scuseria, M.A. Robb, J.R. Cheeseman, V.G. Zakrzewski, J.A.M. Jr., R.E. Stratmann, J.C. Burant, S. Dapprich, J.M. Millam, A.D. Daniels, K.N. Kudin, M.C. Strain, O. Farkas, J. Tomasi, V. Barone, M. Cossi, R. Cammi, B. Mennucci, C. Pomelli, C. Adamo, S. Clifford, J. Ochterski, G.A. Petersson, P.Y. Ayala, Q. Cui, K. Morokuma, P. Salvador, J.J. Dannenberg, D.K. Malick, A.D. Rabuck, K. Raghavachari, J.B. Foresman, J. Cioslowski, J.V. Ortiz, A.G. Baboul, B.B. Stefanov, G. Liu, A. Liashenko, P. Piskorz, I. Komaromi, R. Gomperts, R.L. Martín, D.J. Fox, T. Keith, M.A. Al-Laham, C.Y. Peng, A. Nanayakkara, M. Challacombe, P.M.W. Gill, B. Johnson, W. Chen, M. W. Wong, J.L. Andres, C. Gonzalez, M. Head-Gordon, E.S. Replogle, J.A. Pople, *Gaussian 98, Revision A.11*, Gaussian, Inc., Pittsburgh, PA, 2001.
- [79] G. Brinkmann, O.D. Friedrichs, A. Dress, T. Harmuth, *Match-Commun. Math. Comput. Chem.* 36 (1997) 233.
- [80] P.W. Fowler, D.E. Manolopoulos, *An Atlas of Fullerenes*, Oxford University Press, Oxford, 1995.
- [81] P.W. Fowler, P. Hansen, D. Stevanovic, *Les Cahiers du GERARD G* 34 (2002) 1.
- [82] H.W. Kroto, *Nature* 329 (1987) 529.
- [83] P.W. Fowler, *Contemp. Phys.* 37 (1996) 235.

- [84] P.W. Fowler, T. Heine, D. Mitchell, G. Orlandi, R. Schmidt, G. Seifert, F. Zerbetto, *J. Chem. Soc. Faraday Trans.* 92 (1996) 2203.
- [85] E. Albertazzi, C. Domene, P.W. Fowler, T. Heine, G. Seifert, C.V. Alsenow, F. Zerbetto, *Phys. Chem. Chem. Phys.* 1 (1999) 2913.
- [86] T.G. Schmalz, W.A. Seitz, D.J. Klein, G.E. Hite, *J. Am. Chem. Soc.* 110 (1988) 1113.
- [87] A. Ayuela, P.W. Fowler, D. Mitchell, R. Schmidt, G. Seifert, F. Zerbetto, *J. Phys. Chem.* 100 (1996) 15634.
- [88] E.E.B. Campbell, P.W. Fowler, D. Mitchell, F. Zerbetto, *Chem. Phys. Lett.* 250 (1996) 544.
- [89] J.C. Grossman, L. Mitas, K. Raghavachari, *Phys. Rev. Lett.* 75 (1995) 3870.
- [90] R.O. Jones, G. Seifert, *Phys. Rev. Lett.* 79 (1997) 443.
- [91] M. Saito, Y. Miyamoto, *Phys. Rev. Lett.* 87 (2001) 035503.
- [92] C. Allison, K.A. Beran, *J. Mol. Struct. (THEOCHEM)* 680 (2004) 59.
- [93] W. An, Y. Gao, S. Bulusu, X.C. Zeng, *J. Chem. Phys.* 122 (2005) 204109.
- [94] S. Díaz-Tendero, M. Alcamí, F. Martín, *Chem. Phys. Lett.* 407 (2005) 153.
- [95] L. Zhechkov, T. Heine, G. Seifert, *J. Phys. Chem. A* 108 (2004) 11733.
- [96] X. Lu, Z. Chen, W. Thiel, P. Schleyer, R. Huang, L. Zheng, *J. Am. Chem. Soc.* 126 (2004) 14871.
- [97] S. Díaz-Tendero, F. Martín, M. Alcamí, *Chem. Phys. Chem.* 6 (2005) 92.
- [98] X. Zhao, *J. Phys. Chem. B* 109 (2005) 5267.
- [99] M. Buhl, A. Hirsch, *Chem. Rev.* 101 (2001) 1153.
- [100] W. Qian, M.D. Bartberger, S.J. Pastor, K.N. Houk, C.L. Wilkins, Y. Rubin, *J. Am. Chem. Soc.* 122 (2000) 8333.
- [101] W. Qian, S. Chuang, R.P. Amador, T. Jarrosson, M. Sander, S. Pieniazek, S.I. Khan, Y. Rubin, *J. Am. Chem. Soc.* 125 (2003) 2066.
- [102] G. Sánchez, S. Díaz-Tendero, M. Alcamí, F. Martín, in preparation.
- [103] J.A. Zimmerman, J.R. Eyler, S.B.H. Bach, S.W. McElvany, *J. Chem. Phys.* 94 (1991) 3556.
- [104] S.W. McElvany, S.B.H. Bach, *Proceedings of the 39th ASMS Conference on Mass Spectrometry and Allied Topics* 39 (1991) 422.
- [105] M.S. Baba, T.S.L. Narasimhan, R. Balasubramanian, C.K. Mathews, *Int. J. Mass Spectrom. Ion Process.* 114 (1992) R1.
- [106] D. Muigg, P. Scheier, K. Becker, T.D. Märk, *J. Phys. B* 29 (1996) 5193.
- [107] H. Steger, J. Devries, B. Kamke, W. Kamke, T. Drewello, *Chem. Phys. Lett.* 194 (1992) 452.
- [108] H. Kietzmann, R. Rochow, G. Gantefor, W. Eberhardt, K. Vietze, G. Seifert, P.W. Fowler, *Phys. Rev. Lett.* 81 (1998) 5378.
- [109] B.L. Zhang, C.Z. Wang, K.M. Ho, C.H. Xu, C.T. Chan, *J. Chem. Phys.* 97 (1992) 5007.